

An experimental and computational study of the effect of aqueous solution on the multiphoton ionisation photoelectron spectrum of phenol

Alice Henley,^{‡a} Jamie W. Riley,^{‡a} Bingxing Wang^{a,b} and Helen H. Fielding^{*a}

^a *Department of Chemistry, University College London, 20 Gordon Street, London, WC1H 0AJ, UK*

^b *Present address: College of Chemistry and Chemical Engineering, Henan Institute of Science and Technology, Eastern Hualan Avenue, Xinxiang, 453003, China*

E-mail: h.h.fielding@ucl.ac.uk

[‡]These authors contributed equally to this work.

^{*}To whom correspondence should be addressed

Supplementary Information

Contents

1	Experimental details	2
1.1	Streaming potential measurement	2
1.2	Photoelectron spectra plotted as a function of eKE	3
1.3	Gaussian fitting of the 235.5 nm PES	6
2	Computational details	7
2.1	Convergence of VIE	7
2.2	Calculated and experimental VIEs	8
2.3	Calculated and experimental VEEs	9
2.4	Selecting probable configurations	10
2.5	Investigating inconsistencies between software packages	10
2.6	Orbitals	11
2.7	Coordinates of QM region	14

1 Experimental details

1.1 Streaming potential measurement

The streaming potential was measured using the method described in Ref. 1, based on one reported by Tang *et al.*² Briefly, we recorded the 2 + 1 REMPI of Xe at 249.7 nm in the presence of the liquid-jet. The electron kinetic energy (eKE) is plotted in Fig. S1 as a function of distance from the liquid-jet, Δx .

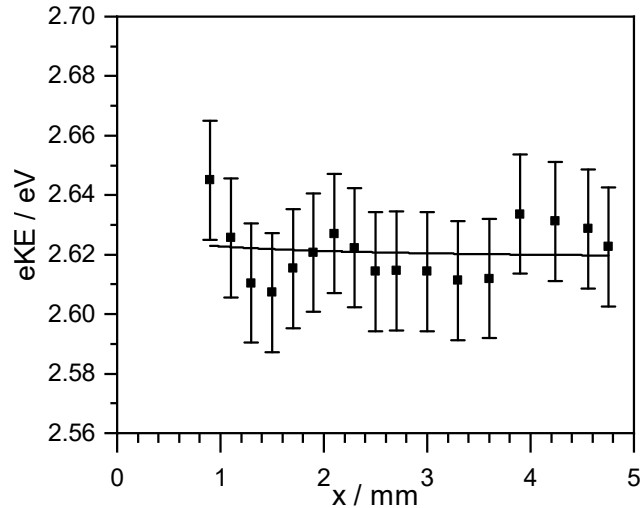


Figure S1: Photoelectron eKE measured following 2 + 1 REMPI of Xe at 249.7 nm in the presence of a liquid-microjet of 100 mM phenol and 30 mM NaF, plotted as a function of distance x between the ionisation point and the liquid-microjet. Measured eKEs correspond to the $\text{Xe}(^1\text{S}_0) \rightarrow \text{Xe}^+(^2\text{P}_{3/2})$ ionisation process. Measurements are fitted using $eKE(x) = eKE_{\text{field-free}} - L\phi_{\text{str}}/(L + \Delta x) + V$, where L is the distance between the ionisation point and the skimmer, $eKE_{\text{field-free}}$ is the eKE following 2+1 photoionisation of Xe when the jet is not running, ϕ_{str} is the streaming potential and V accounts for additional fields in the magnetic bottle spectrometer with the liquid-microjet nozzle in place. Here, $L = 1.05$ mm and $\phi_{\text{str}} \sim 0$ eV. V was determined separately¹ to be $V = -0.06 \pm 0.03$ eV for this work. It has been accounted for in our raw photoelectron spectra. Error bars represent the mean maximum deviations in $eKE(x)$ from the fitted lines from two separate data sets.

1.2 Photoelectron spectra plotted as a function of eKE

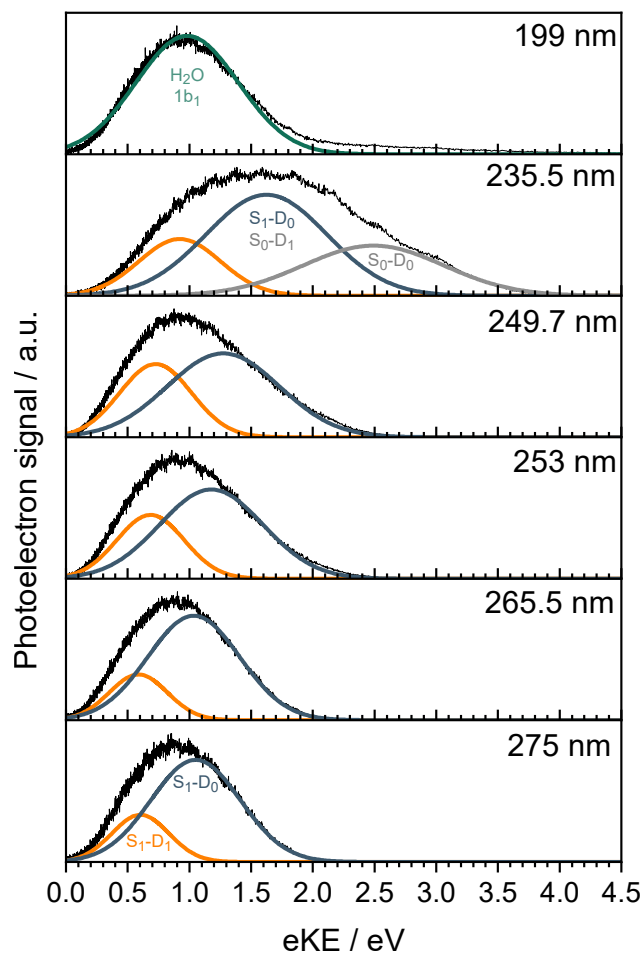


Figure S2: 1+1 UV PES of phenol in aqueous solution recorded following photoexcitation at 275 nm (4.51 eV), 265.5 nm (4.67 eV), 253 nm (4.90 eV), 249.7 nm (4.97 eV), 235.5 nm (5.27 eV) and 199 nm (6.23 eV), plotted as a function of eKE. Gaussian fits correspond to $S_1(1^1\pi\pi^*)-D_0$ (dark blue), $S_1(1^1\pi\pi^*)-D_1$ (orange), S_0-D_0 (light grey) and two-photon ionisation from the $1b_1$ molecular orbital of H_2O (l) (dark green). The S_0-D_1 ionisation process overlaps with the $S_1(1^1\pi\pi^*)-D_0$ process in the 235.5 nm PES.

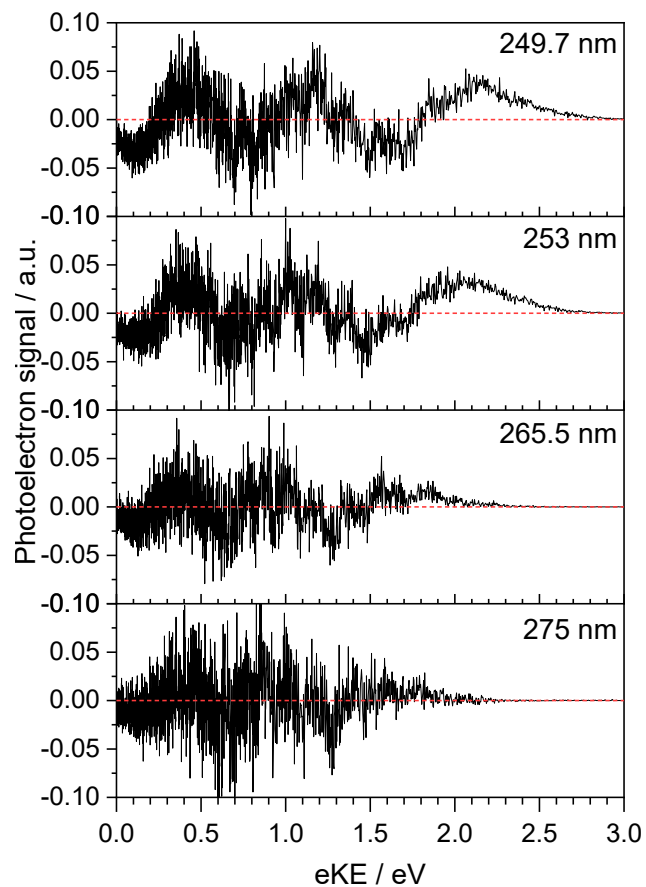


Figure S3: Residuals of Gaussian fits shown in Figure S2 for 275 nm (4.51 eV), 265.5 nm (4.67 eV), 253 nm (4.90 eV) and 249.7 nm (4.97 eV). The positive residual at high eKE has been assigned to S_0 - D_0 and grows in as photon energy increases and the cross-section for absorption to the $1^1\pi\pi^*$ state decreases (see Figs 1 and 3 of main text). The residual for 235.5 nm is discussed below in Fig. S5.

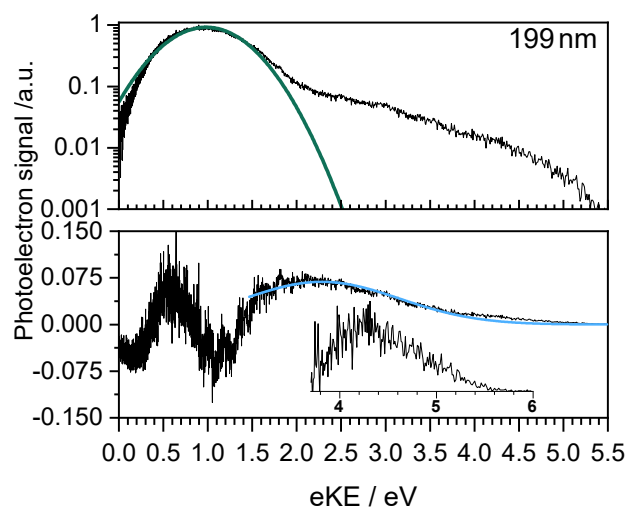


Figure S4: Upper panel shows 1 + 1 UV PES of phenol in aqueous solution recorded following photoexcitation at 199 nm (6.23 eV). The photoelectron signal has been shown on a logarithmic scale to highlight signal at high eKE. The dark green Gaussian has been assigned to two-photon ionisation from the $1b_1$ molecular orbital of H_2O (1). Lower panel shows residual of the Gaussian fit which is assigned to the photoelectron spectrum of the solvated electron. The residual of the residual (inset) is assigned to the S_0 - D_0 photoelectron spectrum.

1.3 Gaussian fitting of the 235.5 nm PES

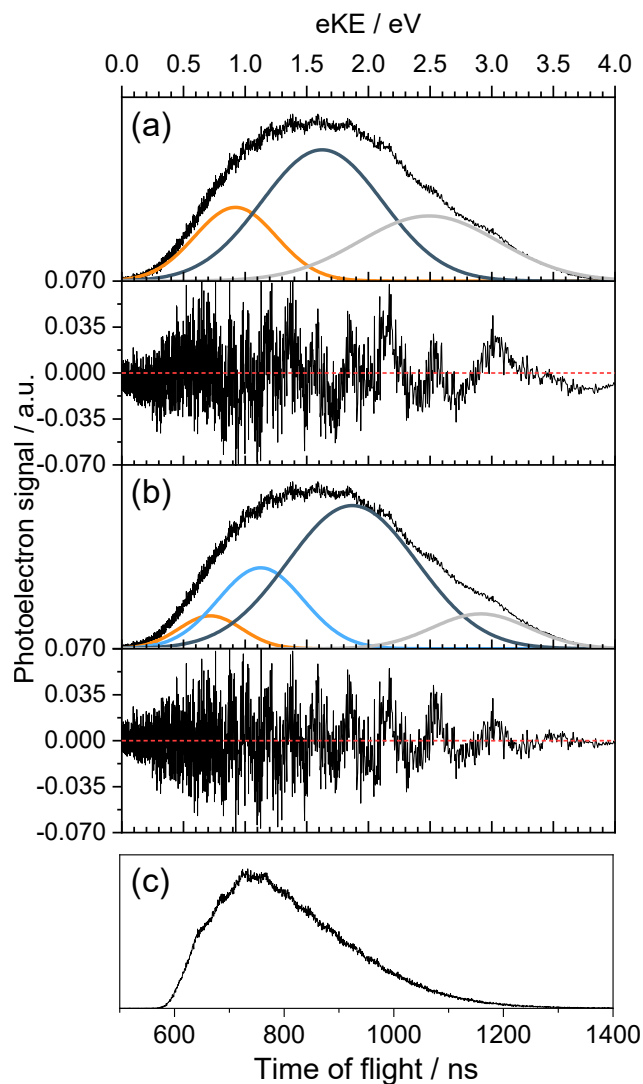


Figure S5: 1+1 UV PES of phenol in aqueous solution recorded following photoexcitation at 235.5 nm (5.27 eV) normalised to maximum photoelectron counts. (a) Plotted as a function of eKE showing a three Gaussian fit corresponding to $S_1(1^1\pi\pi^*)\text{-D}_0$ (dark blue), $S_1(1^1\pi\pi^*)\text{-D}_1$ (orange) and $S_0\text{-D}_0$ (light grey). The residual is shown directly below on the same scale. (b) Plotted as a function of eKE showing a four Gaussian fit corresponding to $S_1(1^1\pi\pi^*)\text{-D}_0$ (dark blue), $S_1(1^1\pi\pi^*)\text{-D}_1$ (orange), $S_0\text{-D}_0$ (light grey) and $e^-(\text{aq}) \rightarrow e^-(\text{g})$ (light blue). The residual is shown below directly below on the same scale. (c) Plotted as a function of time of flight to show the origin of the oscillations in the spectrum, which are enhanced by the Jacobian transformation to eKE.

2 Computational details

2.1 Convergence of VIE

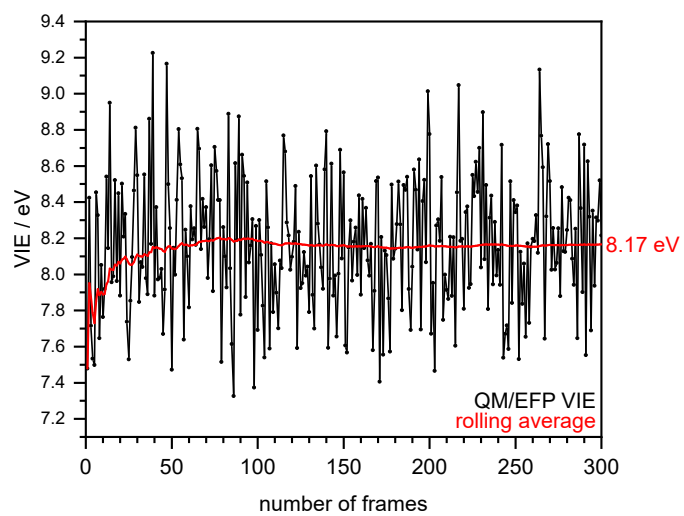


Figure S6: Convergence of VIE of the $[\text{phenol}\cdot(\text{H}_2\text{O})_5]_{\text{QM}}[(\text{H}_2\text{O})_{n\geq 250}]_{\text{EFP}}$ system calculated with B3LYP/aug-cc-pvdz over randomly ordered trajectory frames.

2.2 Calculated and experimental VIEs

	S ₀ -D ₀	S ₀ -D ₁
Experiment		
Fitted peak maxima (Fig. 3 in paper)	8.0 ± 0.1	8.9 ± 0.1
Roy <i>et al.</i> (ref. 3)	8.0 ± 0.1	8.5 ± 0.1
Ghosh <i>et al.</i> (ref. 4)	7.8 ± 0.1	8.6 ± 0.1
Calculations		
[phenol] _{QM} [(H ₂ O) _{bulk}] _{EFP} (ref. 4) QM = EOM-IP-CCSD/6-31+G*	7.9	8.6
[phenol·(H₂O)₅]_{QM}[(H₂O)_{n≥250}]_{EFP}		
B3LYP/aug-cc-pvdz (average of 300)	8.17	
B3LYP/aug-cc-pvdz (average of 10)		
unoptimised	8.24	
QM/EFP optimised	7.93	
B3LYP/6-31+G* (average of 10)		
unoptimised	8.25	
QM/EFP optimised	7.94	
EOM-IP-CCSD/6-31+G* (average of 10)		
unoptimised	8.64	9.23
QM/EFP optimised	8.29	9.19

Table S1: Measured and calculated VIEs from S₀ to D₀ (electron hole in π_{HOMO}) and S₀ to D₁ (electron hole in π_{HOMO-1}) for phenol in aqueous solution. VIEs calculated using [phenol·(H₂O)₅]_{QM}[(H₂O)₂₅₀₋₃₀₀]_{EFP} are presented as averages of all 300 frames taken from the molecular dynamics sampling, or averages over the ten configurations with S₀ energies closest to the average S₀ energy (see Section 2.4). Unoptimised structures are taken directly from the molecular dynamics sampling whereas the QM/EFP optimised structures have been optimised at the QM/EFP (PBE0/aug-cc-pvdz) level. All values are in eV.

2.3 Calculated and experimental VEEs

	S ₀ -S ₁ VEE
Gas-phase	
Experiment ^a	4.63
Experiment (ref. 5)	4.51
EOM-EE-CCSD/aug-cc-pvdz (ref. 6)	4.87
ADC(2)/aug-cc-pvdz (ref. 7)	4.86
EOM-EE-CCSD/6-31+G*	5.06
ADC(2)/6-31+G*	5.06
Aqueous solution	
experiment ^a	4.57
phenol·(H ₂ O) ₃ DF-CC2/aug-cc-pvtz AEE (ref. 8)	4.56
[phenol·(H ₂ O)] _{QM} [(H ₂ O) _{bulk}] _{MM} (ref. 7)	4.85
EOM-EE-CCSD/6-31+G*	
unoptimised	5.03
QM/EFP optimised	5.04
ADC(2)/6-31+G*	
unoptimised	5.03
QM/EFP optimised	5.03

Table S2: Measured and calculated VEEs from S₀ to S₁ ($\pi_{HOMO} \rightarrow \pi^*$) for phenol in the gas phase and in aqueous solution. For the QM/EFP approaches, an average over the ten configurations of [phenol·(H₂O)₅]_{QM}[(H₂O)₂₅₀₋₃₀₀]_{EFP} with S₀ energies closest to the mean S₀ energy are presented (see Section 2.4). Unoptimised structures are taken directly from the molecular dynamics sampling whereas the QM/EFP optimised structures have been optimised at the PBE0(aug-cc-pvdz)/EFP level. All values are in eV.

^aEstimated from the maximum of the UV-vis absorption spectrum presented in Fig. 1 of the main text.

2.4 Selecting probable configurations

For each of the 300 configurations obtained from the MD trajectory, the energy of the S_0 state was calculated using QM/EFP (B3LYP/aug-cc-pvdz) where the QM region consisted of phenol and the five closest water molecules to any atom within the phenol molecule and the EFP region consists of the water molecules within 10 Å of any atom within the phenol molecule (250-300 EFP water molecules). The distribution of the S_0 energies is shown in Fig. S7.

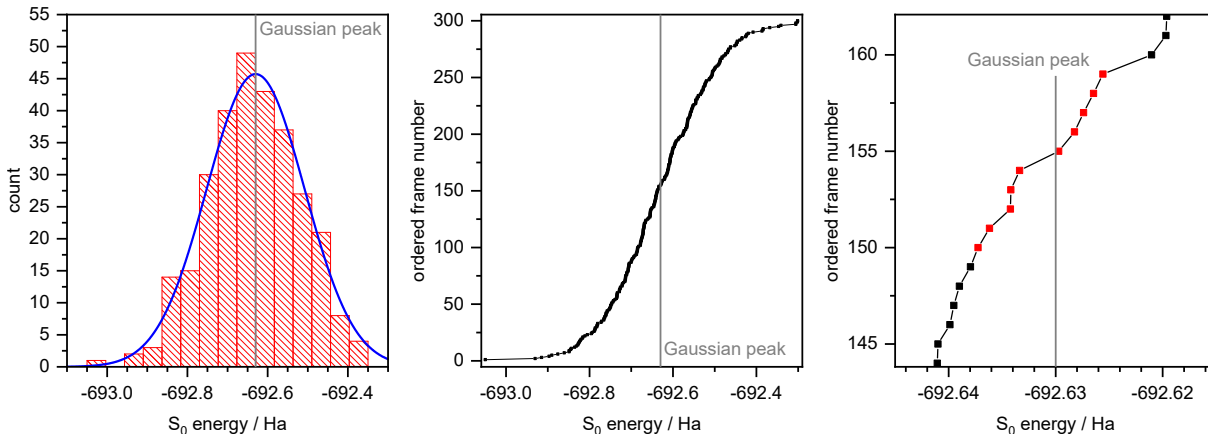


Figure S7: Left: distribution of S_0 energies calculated using QM/EFP (B3LYP/aug-cc-pvdz) plotted as a histogram with bin size 0.04667 Ha. A Gaussian is fitted to this distribution (blue line). Middle: the 300 QM/EFP frames ordered by S_0 energy calculated using QM/EFP (B3LYP/aug-cc-pvdz). Right: an expansion of the middle plot highlighting in red the ten selected configurations with energies close to the S_0 energy at the peak of the Gaussian fit. In all plots, the peak of the Gaussian fit is identified by a vertical grey line.

It is likely that frames with S_0 energies close to the average S_0 energy will be probable configurations of the phenol-bulk water system at 300 K. In order to select frames with S_0 energies close to the average S_0 energy, a Gaussian fit is first used to find this average energy. Then the frames were ordered with increasing S_0 energy and the ten frames with S_0 energies closest to this average energy were selected. These frames were then used in higher-level theory calculations and QM/EFP geometry optimisations.

2.5 Investigating inconsistencies between software packages

Throughout this work, various quantum chemistry software packages were used which each have different algorithms for calculating energies and optimising structures. To investigate the possibility of any inconsistencies in geometry optimisations, we have optimised gas-phase phenol at the PBE0/aug-cc-pvdz and B3LYP/aug-cc-pvdz levels in both Gaussian09 and Firefly. All four structures are identical by observation and, following alignment, the cartesian coordinates only differ by <0.001 Å. Comparing just the two PBE0 structures gave an RMSD (root-mean-square deviation) of 0.0004 Å while that of the B3LYP structures gave an RMSD of 0.001 Å. Additionally, to compare the absolute energies obtained in Gaussian09 and QChem, we have calculated the electronic energy of gas-phase phenol (optimized using B3LYP/6-311++G(3df,3pd)) in the two software packages at the B3LYP/aug-cc-pvdz level. The energies differed by <0.001 eV.

2.6 Orbitals

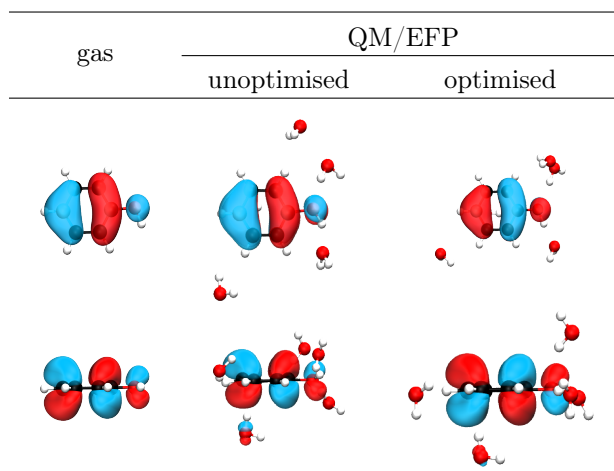


Table S3: D_0 hole orbitals (π_{HOMO}) taken from gas-phase and QM/EFP calculations at the EOM-IP-CCSD/6-31+G* level. QM/EFP orbitals shown are those corresponding to the configuration with S_0 energy closest to the Gaussian fit peak (see Section 2.4).

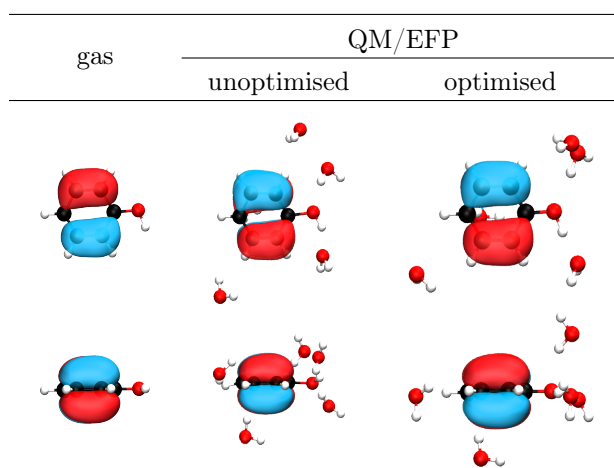


Table S4: D_1 hole orbitals (π_{HOMO-1}) taken from gas-phase and QM/EFP calculations at the EOM-IP-CCSD/6-31+G* level. QM/EFP orbitals shown are those corresponding to the configuration with S_0 energy closest to the Gaussian fit peak (see Section 2.4).

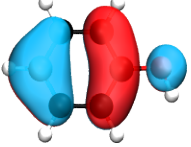
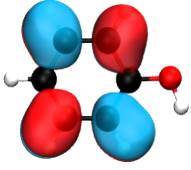
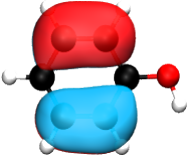
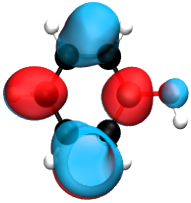
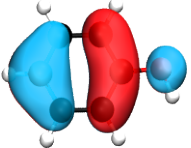
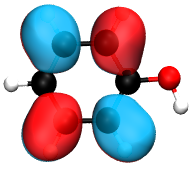
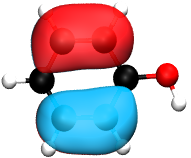
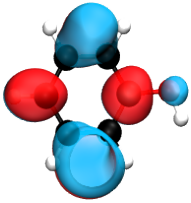
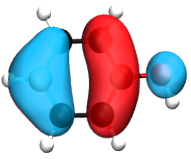
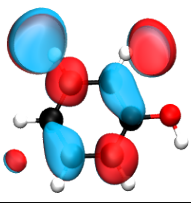
method		occupied orbital		unoccupied orbital	c^2	
ADC(2)	π_{HOMO}		→	π_1^*		67
	π_{HOMO-1}		→	π_2^*		15
EOM-EE-CCSD	π_{HOMO}		→	π_1^*		56
	π_{HOMO-1}		→	π_2^*		17
	π_{HOMO}		→	π_3^*		6

Table S5: Orbital contributions found for the $S_0 \rightarrow S_1$ transition in VEE calculations for isolated phenol in the gas phase. Weights (c^2) are given in % and the 6-31+G* basis set was used with both methods.

structure	occupied orbital	unoccupied orbital	c^2
unoptimised	π_{HOMO}	$\rightarrow \pi_1^*$	24
optimised	π_{HOMO}	$\rightarrow \pi_1^*$	30
	π_{HOMO}	$\rightarrow \pi_2^*$	23

Table S6: Orbital contributions found for the $S_0 \rightarrow S_1$ transition in ADC(2)/6-31+G* QM/EFP calculations for phenol in bulk water in the unoptimised (directly from the MD trajectory) and QM/EFP optimised geometry for the configuration with S_0 energy closest to the Gaussian fit peak (see Section 2.4). Weights (c^2) are given in %.

2.7 Coordinates of QM region

atom	unoptimised / Å			optimised with QM/EFP / Å		
	<i>x</i>	<i>y</i>	<i>z</i>	<i>x</i>	<i>y</i>	<i>z</i>
C	-2.306042	3.591157	6.307538	-2.485810	3.437451	6.843126
H	-2.214230	4.203257	7.145574	-2.409805	3.933824	7.809118
C	-1.781224	4.103748	5.098080	-2.101370	4.083194	5.664169
H	-1.187908	5.024688	5.090264	-1.718931	5.103159	5.697571
C	-3.251530	2.565712	6.268416	-2.967666	2.130077	6.769525
H	-3.812224	2.265480	7.111988	-3.270673	1.620367	7.679542
C	-2.052229	3.347309	3.948592	-2.209449	3.440845	4.434100
H	-1.585507	3.688072	3.006372	-1.919061	3.945631	3.514193
C	-3.536026	1.897261	5.098533	-3.077323	1.472918	5.547190
H	-4.306682	1.174718	5.057335	-3.466452	0.456907	5.498383
C	-2.903544	2.274796	3.970664	-2.702521	2.132166	4.370221
O	-3.150139	1.705652	2.654387	-2.796677	1.541559	3.155670
H	-3.507242	0.802591	2.702881	-3.248370	0.650431	3.219682
O	-2.865253	3.527121	-0.535025	-2.275059	3.248347	0.890503
H	-2.736118	2.924174	-1.296454	-2.334658	2.603530	1.613432
H	-3.640584	3.160995	-0.071704	-3.124912	3.162421	0.428681
O	-4.550243	5.557623	5.587215	-5.468073	4.167769	6.041751
H	-4.785477	5.387511	4.677302	-5.671016	3.751265	5.190431
H	-4.025469	4.754822	5.777183	-4.513971	4.044582	6.146559
O	-3.622339	-0.893667	3.669677	-4.013344	-0.779217	3.242567
H	-3.547246	-1.834778	3.833649	-3.822395	-1.442011	3.924923
H	-4.563444	-0.748183	3.967450	-4.974754	-0.650612	3.297636
O	-4.358450	1.242101	9.543933	-3.463510	2.479051	10.219063
H	-4.069477	2.029460	9.076242	-4.407703	2.654371	10.184001
H	-4.011615	0.473106	9.014648	-3.363649	1.554880	9.934894
O	1.116907	3.593470	1.328483	0.765121	2.629333	1.294168
H	1.516525	3.006933	1.970852	1.473993	2.440063	1.929492
H	0.489448	4.005100	1.949899	0.284537	3.356137	1.708311

Table S7: Cartesian coordinates of the QM region of the [phenol·(H₂O)₅]_{QM}[(H₂O)_{*n*≥250}]_{EFP} system used in QM/EFP calculations for the configuration with S₀ energy closest to the Gaussian fit peak (see Section 2.4). Both unoptimised, *i.e.* taken directly from the MD trajectory, and optimised (QM/EFP PBE0/aug-cc-pvdz) geometries are listed.

References

- [1] J. W. Riley, B. Wang, M. A. Parkes and H. H. Fielding, *Rev. Sci. Instrum.*, 2019, submitted.
- [2] Y. Tang, Y.-i. Suzuki, H. Shen, K. Sekiguchi, N. Kurahashi, K. Nishizawa, P. Zuo and T. Suzuki, *Chem. Phys. Lett.*, 2010, **494**, 111–116.
- [3] A. Roy, R. Seidel, G. Kumar and S. E. Bradforth, *J. Phys. Chem. B*, 2018, **122**, 3723–3733.
- [4] D. Ghosh, A. Roy, R. Seidel, B. Winter, S. Bradforth and A. I. Krylov, *J. Phys. Chem. B*, 2012, **116**, 7269–7280.
- [5] S. Karmakar, D. P. Mukhopadhyay and T. Chakraborty, *J. Chem. Phys.*, 2015, **142**, 184303.
- [6] J. W. Riley, B. Wang, J. L. Woodhouse, M. Assmann, G. A. Worth and H. H. Fielding, *J. Phys. Chem. Lett.*, 2018, **9**, 678–682.
- [7] I. Sandler, J. J. Nogueira and L. González, *Phys. Chem. Chem. Phys.*, 2019, DOI: 10.1039/c8cp06656f.
- [8] D. Schemmel and M. Schütz, *J. Chem. Phys.*, 2007, **127**, 174304.